

Electromagnetic Scattering from Grassland—Part II: Measurement and Modeling Results

James M. Stiles, Kamal Sarabandi, *Senior Member, IEEE*, and Fawwaz T. Ulaby, *Fellow, IEEE*

Abstract—The validity of a coherent, grassland scattering model is determined by comparing the model predictions with direct measurements of a representative grass canopy. A wheat field was selected as the test target, and polarimetric, multifrequency backscattering data were collected over an entire growing season, along with a complete set of ground-truth data. The L-band measured data demonstrated a strong dependence on azimuthal look direction in relation to the row direction of the wheat. The C-band measurements likewise showed an interesting backscattering response, wherein σ_{vv}^0 actually increased with incidence angle for many cases.

The coherent scattering model provides backscattering data that match and predict these measured data and most of the other measured data well. The model shows that at L-band, the incoherent scattering power alone is insufficient for predicting the measured results, as the coherent terms can dominate the total scattered energy. Additionally, the model, which accounts for this nonuniform illumination of the wheat elements, demonstrates the peculiar data observed for C-band. Likewise, it is demonstrated that the fidelity used to model grass constituents (e.g., curvature) is required to match the scattering measurements accurately.

Index Terms—Microwave scattering from grasslands, vegetation scattering measurements.

I. INTRODUCTION

OVER THE course of a single growing season, an experiment was conducted at a site near Ann Arbor, MI, to measure and quantify the microwave scattering from a representative grassland canopy. Wheat vegetation was selected as the test target, as wheat continuously and dramatically changes form (e.g., height, moisture, structure) during its brief growing period, thus providing a disparate set of scattering targets over a growing season. Using a multifrequency (L-, C-, and X-band), scatterometer built at the Radiation Laboratory, University of Michigan, Ann Arbor (Table I) [1], polarimetric scattering data were collected from this test site as a function of frequency, incidence angle, and azimuth look angle. Along with the scattering data, a thorough set of ancillary measurements, precisely describing the grass canopy, was collected (Table II). Rather than collecting only the ground-truth data of interest to the user of the remotely-sensed measurements (e.g., moisture, biomass, leaf area, etc.), all parameters that affect microwave scattering were measured. For example, leaf curvature and cross-section may be

TABLE I
SCATTEROMETER SPECIFICATIONS

Parameter	Value	Units
Center Frequency		GHz
L-band	1.25	
C-band	5.3	
X-band	9.5	
Bandwidth		MHz
L-band	300	
C-band	400	
X-band	500	
Antenna Beamwidth		degrees
L-band	12.0	
C-band	8.0	
X-band	5.4	
Antenna Gain		dB
L-band	22.1	
C-band	25.3	
X-band	29.5	
X-pol Isolation †		dB
L-band	22	
C-band	26	
X-band	29	

† prior to calibration

of little or no ultimate interest, yet these parameters were quantified as they presumably affect plant scattering. The goal in collecting this complete data set was to eliminate the unknown or “free” input parameters when evaluating scattering-model performance.

One of the goals of this study was to add to the existing data set on scattering from wheat and grass targets [2]–[7]. However, the primary use of this specific data set was to provide a basis for evaluating the performance of a high-fidelity, phase-coherent grassland scattering model. For example, one primary goal was to determine the significance, if any, of the coherent terms that arise if the scattering is considered in a phase-coherent manner. Included in these terms are the scattered field correlations between dissimilar elements and likewise, between dissimilar plants (i.e., row structure). Another goal was to determine the effect of plant structure on scattering response, as the high-fidelity scattering model also allows for the precise modeling of canopy elements, including complex curvatures and cross-section shapes. Several previous studies have used simpler element structures in the evaluation of grass vegetation, such as

Manuscript received November 14, 1997; revised November 10, 1998.

J. M. Stiles is with the Radar Systems and Remote Sensing Laboratory, University of Kansas, Lawrence, KS 66045-2969 USA (e-mail: jstiles@rsl.ukans.edu).

K. Sarabandi and F. T. Ulaby are with the The Radiation Laboratory, University of Michigan, Ann Arbor, MI 48109 USA.

Publisher Item Identifier S 0196-2892(00)00401-0.

TABLE II
VARIOUS PARAMETERS DESCRIBING THE TEST VEGETATION AND SOIL. ALL PARAMETERS ARE USED IN THE SCATTERING MODEL. THE LEAF PARAMETERS ARE DEFINED IN PART I OF THIS PAPER

Parameter	Value	Units
Canopy Parameters		
Plant Density	427.4	plants/square meter
Row Density	82.7	plants/row meter
Row Spacing X_{row}	19.4	cm
x-deviation σ_x	1.2	cm
Soil Parameters		
RMS Height	0.31	cm
Bulk Density	1.34	g/cc
Soil Type	Sandy Loam	
Leaf Parameter		
blade thickness t	0.02	cm
blade width w	1.12	cm
blade curvature	0.01	na
leaf angle θ	5.0	degrees
c_1 mean	3.81	na
c_2 mean	0.567	na
ρ_0 mean	8.89	cm
c_1 variance	1.08	na
c_2 variance	0.036	na
ρ_0 variance	6.66	cm
$c_1 c_2$ covariance	0.133	na
$c_1 \rho_0$ covariance	-1.552	na
$\rho_0 c_2$ covariance	-0.045	na

straight elements with circular cross-sections [8]–[11]. The extent to which these structural parameters actually affect the scattered response is an important issue for this study.

Additionally, we wish to determine a better understanding of the individual scattering mechanisms that constitute the overall scattering response of grassland canopies. For example, we wish to understand better the relative contribution of scattering terms that are sensitive to soil moisture (direct surface scattering), those that are sensitive to the vegetation (direct canopy scattering), and those that are sensitive to both (ground-reflection terms). The relative importance of these different scattering terms for various incidence angles and polarizations will be examined.

II. L-BAND RESULTS

The antenna mount of the scatterometer system allowed for data to be collected as a function of azimuth as well as elevation angle. In general, due to the row structure of the wheat canopy, the measured scattering data exhibited a strong dependence on azimuth look angle, with significant changes from at least -40° to 40° (0° corresponding to an azimuthal look direction perpendicular to row direction). The variation is similar to a $\sin x/x$ pattern and suggests a coherent effect in the data. Another interesting behavior is the fact that this variation is quite dependent

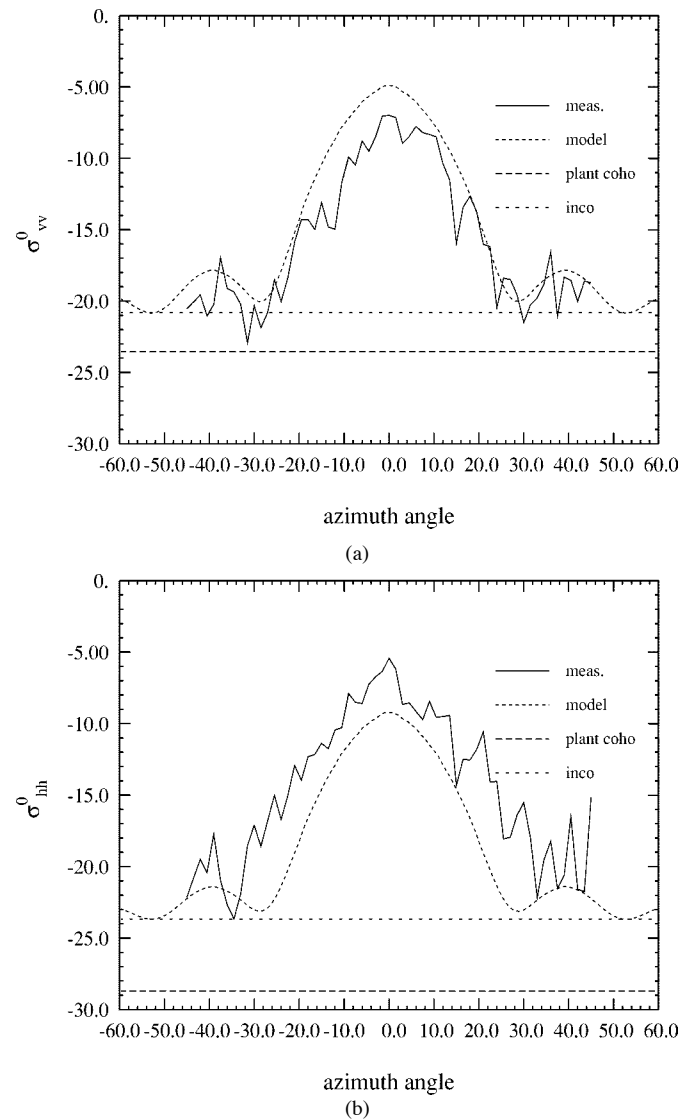


Fig. 1. Typical (May 25) L-band measured and modeled backscattering (σ_{vv} and σ_{hh}) as a function of azimuth angle. Curves are provided for the total incoherent backscattered power (inco), the total when correlation between dissimilar scattering mechanisms is added (+ mech cor), the total when the correlation between dissimilar plant elements is further added (+ element cor), and the total backscattered power when all coherent effects, including row structure, are determined (total).

on incidence angle, with the maximum backscattering value occurring at 40° incidence and then dropping rapidly as the incidence angle increases. This provides more evidence of a coherent effect, as the first Bragg mode for a periodic scatterer with the wheat-row spacing (20 cm) is approximately 40° at L-band. At larger azimuth angles, where the sensor is no longer perpendicular to the row direction, the dependence on elevation angle is less dramatic, suggesting that the coherent effect of the row structure has less importance to the overall scattering behavior.

For example, Fig. 1 shows the measured and modeled backscattering for a wheat canopy early in the growing season (Table III) at an incidence angle of 40° , as a function of azimuth angle. The illuminated area was approximately 1 m in diameter, which included portions of about six rows of wheat plants. The backscattering estimate is poor for these data (i.e., the data are noisy), because the extreme dependence on both azimuth and elevation angle reduces the number of independent samples

TABLE III
VEGETATION PARAMETERS SPECIFIC TO THE VEGETATION OF MAY 25. ALL
PARAMETERS ARE USED IN THE SCATTERING MODEL

Parameter	Value	Units
vol. soil moisture	0.113	na
vol. leaf moisture	0.516	na
vol. stalk moisture	0.580	na
leaf layer thickness	33.5	cm
ave. leaf height	22.7	cm
leaves/plant	4	na
stalk diam.	0.33	cm
stalk height average	39.5	cm
stalk height std. dev.	2.3	cm

available to be averaged. It is evident that the coherent scattering model, when considering all coherent effects including row structure, predicts the backscattering and its dependence on azimuth angle well. However, the true significance of the results is seen when observing the lower two traces of the plots. The lowest trace is that of the incoherent scattered power (that is, the summation of the scattered power from each of the individual elements of the vegetation canopy). This quantity, which is generally used to model the scattering from grass vegetation, is as much as 25 dB in error from the measured data. Also plotted on the graphs is the total plant power (that is, the incoherent summation of the total power: coherent plus incoherent) from each plant (i.e., all coherent effects except row structure). This value includes all the coherent terms resulting from the correlation between dissimilar plant elements and scattering mechanisms. The difference between the total plant power and the incoherent power alone is as much as 5 dB. Therefore, the coherent plant scattering terms are not only significant, but in aggregate, they have a magnitude that is much greater than the incoherent scattering power.

The model thus indicates that the azimuthal dependence of the backscattering data is largely an effect of the coherent response due to row structure. This finding indicates a significant problem when observing row-structured vegetation, as the scattering response is not necessarily linearly proportional to the illumination spot and/or ambiguity function size. As a result, otherwise similar sensors may indicate different backscattering coefficients when observing the same vegetation target. This is especially true when the illumination area is small, as the resulting row coherence effect is significant over a large range of azimuthal angles. Thus, for the scatterometer used in this study, where the diameter of the illuminated area is on the order of a few meters, this row coherence is very significant. For larger resolution sensors, the coherent scattering lobe would be narrower, such that the row coherent effect would occur only when observing the vegetation at an azimuth angle approaching 0° .

The L-band data collected were dependent on both azimuth and elevation angle. Therefore, the response as a function of incidence angle was evaluated at two specific azimuth angles, 0° and 45° . Fig. 2 shows the modeled scattering contributions for a canopy of tall, green wheat as a function of elevation angle, when observed at an azimuth angle of 45° . The lowest curve is

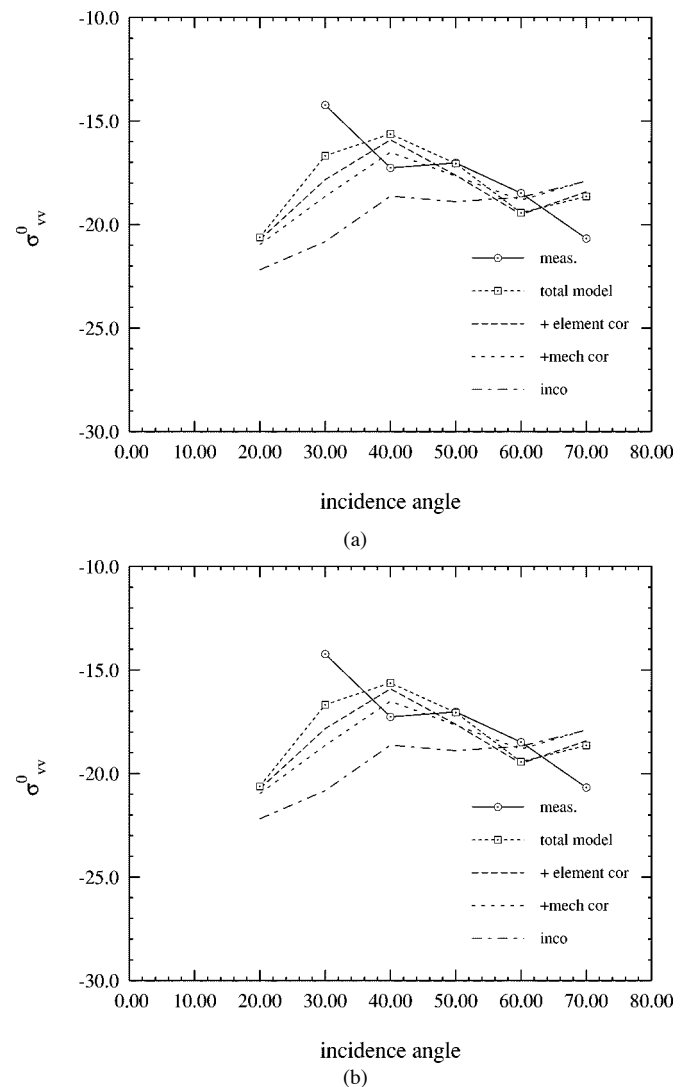


Fig. 2. L-band measured and modeled backscattering (σ_{vv} and σ_{hh}) from a tall, green wheat canopy (June 10) at 45° azimuth, plotted as a function of incidence angle.

again the incoherent power, with the next trace the result after adding the coherent power relating to the correlation between dissimilar scattering mechanisms of a single element. Note that these terms are a significant addition and can increase the scattering power by as much as 2.5 dB. The next curve provides the total power when including the coherent effect resulting from the correlations between dissimilar plant elements, an addition that also increases the total scattered power to as much as 4 dB greater than the incoherent power alone. The final trace shows the total scattered power, including the coherent effects of the row structure. Note that at 45° , the contribution from this phenomenon is relatively small, as this azimuth angle is generally outside of the coherent scattering lobe shown in Fig. 1. Still, the coherent effect of row structure can increase the overall scattered power by almost another 1 dB.

Fig. 3 displays the scattering for the same canopy as Fig. 2, except that the radar is looking perpendicular to the row structure ($\phi_i = 0$). In this case, the coherent effect due to the row structure is the dominant scattering contributor in all but the largest incidence angles. The Bragg scattering effect is evident, peaking at 40° and then falling off rapidly as the

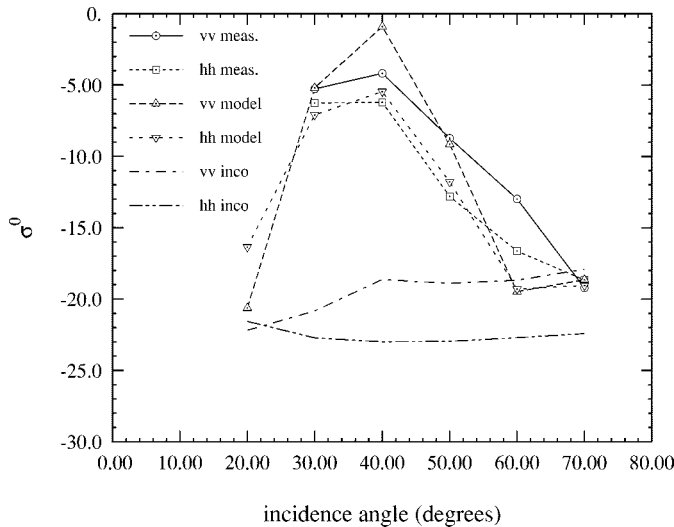


Fig. 3. L-band measured and modeled backscattering from a tall, green wheat canopy (June 10) at 0° azimuth, plotted as a function of incidence angle.

TABLE IV

VEGETATION PARAMETERS SPECIFIC TO THE VEGETATION OF JUNE 10. ALL PARAMETERS ARE USED IN THE SCATTERING MODEL

Parameter	Value	Units
vol. soil moisture	0.229	na
vol. leaf moisture	0.512	na
vol. stalk moisture	0.460	na
vol. grain moisture	0.110	na
grain diam.	0.97	cm
grain length average	7.2	cm
grain length std. dev.	0.77	cm
leaf layer thickness	46.3	cm
ave. leaf height	41.5	cm
leaves/plant	3	na
stalk diam.	0.37	cm
stalk height average	77.2	cm
stalk height std. dev.	4.5	cm

incidence angle increases in both measured and modeled data. The figure likewise displays the incoherent scattering power, and the largest discrepancy between the incoherent power and the total power at this azimuth angle is quite apparent. At an incidence angle of 40° , the measured and modeled data are approximately 15 dB greater than the value of the predicted incoherent scattering power. Numerically, the match between the measured value is relatively large due to the small number of data samples. However, the important result is that the phase-coherent model clearly comprehends the magnitude and response of the measured data better than the incoherent scattering formulation alone. This is a major result of this study, as the incoherent power is generally the only scattering term considered in grassland scattering models.

Beyond presenting the scattering power in terms of the incoherent and coherent scattering results, it is important to examine which of the many scattering terms are significant to the overall scattered power. The sheer number of these terms makes plot-

TABLE V

THE RCS (σ) OF A SINGLE, SORT WHEAT PLANT (WITH NO GRAIN HEAD, MAY 25), LISTED IN TERMS OF THE MAGNITUDE OF THE VARIOUS COHERENT AND INCOHERENT SCATTERING TERMS. THE RCS VALUES ARE IN SQUARE CENTIMETERS (dBscm)

	σ_{hh}	σ_{vv}
total	-9.79	-7.69
leaf inco	-16.66	-18.29
leaf coho	-21.56	-34.37
stalk inco	-20.40	-10.59
stalk coho	-20.08	-13.95
stalk/leaf	-13.95	-15.17
leaf/leaf	-17.66	-27.79

ting the results difficult, so instead, the results will be presented in tabular form. Two test days will be presented (Tables III and IV), both at an incidence angle of 40° . For the early test day (Fig. 1), the wheat was relatively short and no grain head was present. For the second test day (Figs. 2 and Fig. 3), the wheat at its tallest and the grain head had fully emerged. Tables V and VI break down the total radar cross section of a single plant within the grass canopy, providing the incoherent scattering power and the magnitude of the coherent effects for each plant element, as well as the correlation between dissimilar elements.

From Fig. 1, it is evident that the horizontal-copolarized scattering for the early test day is modified by the coherent effects of the plant to a greater extent than are the vertical-polarized backscattering. The model shows that for σ_{vv} , this is due mainly to the correlation in scattering between the stalk and leaf elements (-13.95 dBscm), and correlation between dissimilar leaf elements (-17.66 dBscm). Thus, the scattering from an entire wheat plant is different from the sum of the scattered power from its individual parts, and therefore, an individual plant must be considered in total as a single scattering element. For vertically polarized, copolarized scattering, however, the table shows that the correlation between dissimilar elements is not as significant. The scattering instead is due mainly to the stalk element, with the majority of the coherent scattering attributable to the correlation between dissimilar scattering mechanisms of the stalk element. This is due to the fact that the vertically polarized incident wave couples strongly into the vertical stalks, increasing both the scattering from these elements and the extinction of the coherent incident wave. As a result, the attenuation associated with the propagation path to/from the lower-lying leaves of the plant element is large, and the scattering (both coherent and incoherent) from the leaf elements is diminished.

For the later test data, a grain element had emerged, and the wheat vegetation had reached its maximum height (85 cm). For the horizontally polarized case, the correlation between dissimilar elements is still significant, including the correlation between grain and stalk elements. However, the long stalk element for this test case results in increased scattering from that plant element, and the relative significance of the leaf elements to the overall scattering is less than in the previous case. This is likewise true for the vertically polarized case, where the scattering

TABLE VI
THE rcs (σ) OF A SINGLE, TALL WHEAT PLANT (WITH GRAIN HEAD, JUNE 10), LISTED IN TERMS OF THE MAGNITUDE OF THE VARIOUS COHERENT AND INCOHERENT SCATTERING TERMS. THE rcs VALUES ARE IN SQUARE CENTIMETERS (dBscm)

	σ_{hh}	σ_{vv}
total	-5.35	-2.35
leaf inco	-16.9	-21.21
leaf coho	-19.8	-37.29
stalk inco	-13.25	-6.83
stalk coho	-13.23	-7.11
grain inco	-15.22	-10.32
grain coho	-18.99	-17.86
stalk/leaf	-11.48	-14.5
grain/stalk	-14.38	-12.23
leaf/leaf	-19.89	-30.3

from the stalk element dominates. It is evident that the coherent term resulting from the correlation between grain and stalk element is significant, thus indicating that the scattering from the two elements should not be considered separately.

It should be noted, however, that the computational cost of computing each coherent term is equivalent to a single incoherent term. As a result, the cost of computing all coherent terms can be as much as two orders of magnitude larger than evaluating just the incoherent power. As a result, these values should only be computed if significant compared to the overall scattered power. However, as the results of this section have shown, the incoherent terms can dominate total scattered power for grass canopies and large wavelengths.

As with the copolarized scattered power, the measured cross-polarized data exhibit a strong dependence on azimuth angle. Unlike the copolarized case, however, the model does a poor job in replicating the measured azimuthal response. The first-order scattering model predicts no coherent cross-polarized scattering term from the row structure, and thus, the predicted scattering is independent of incidence angle (Fig. 4). This likely indicates that the cross-polarized response is the result of higher-order scattering terms, which are not included in the model. However, other error sources may exist. For example, the constituent-element scattering models may still be too simple to account for the cross-polarized response resulting from the complex and random structure of natural elements.

III. C-BAND AND X-BAND RESULTS

The C-band radar frequency of 5.3 GHz is more than four times the center frequency of the L-band data. This increase in frequency also greatly increases the electrical size of the wheat plants and their elements, and therefore, the phase of the coherent scattering terms varies greatly over the random variation of the plant structure. As a result, the expected values of the coherent terms are small and insignificant when compared to incoherent scattering data. This includes the coherent terms associated with plant and row structure, so that the predicted scattering value is independent of azimuth angle.

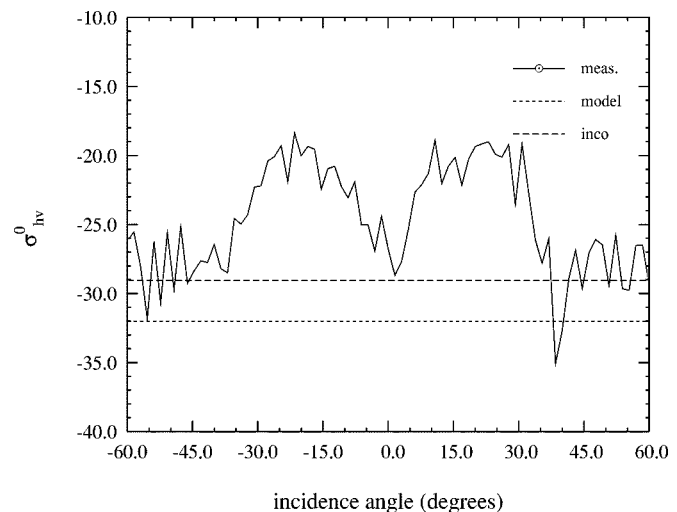


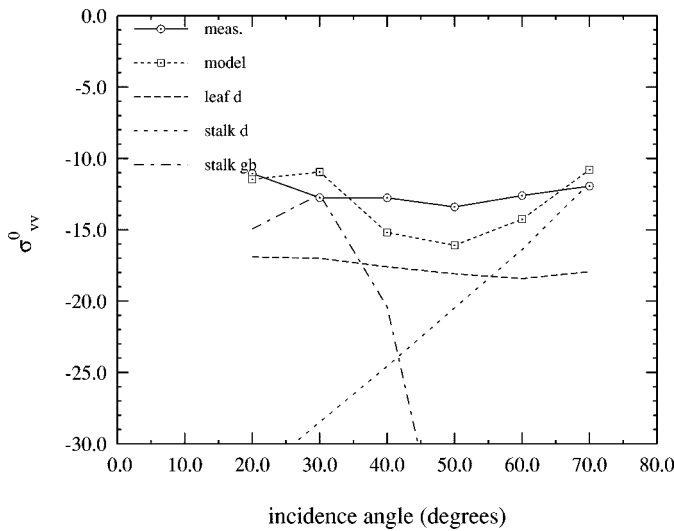
Fig. 4. Typical (May 25) L-band measured and modeled cross-polarized backscattering as a function of azimuth angle.

The measured C-band scattering data, however, revealed an interesting phenomenon when plotted as a function of incidence angle. This general behavior shows σ_{vv}^0 initially decreasing with incidence angle, but then sharply increasing from 40 to 70°. For several test days, the largest value of σ_{vv}^0 actually occurs at 70° incidence. This is in marked contrast to the scattering behavior of most random media, where σ^0 decreases monotonically as a function of incidence angle as σ_{hh}^0 does in this data. However, it appears to be a common phenomenon for wheat scattering, as other authors have reported similar results [4], [7], [12].

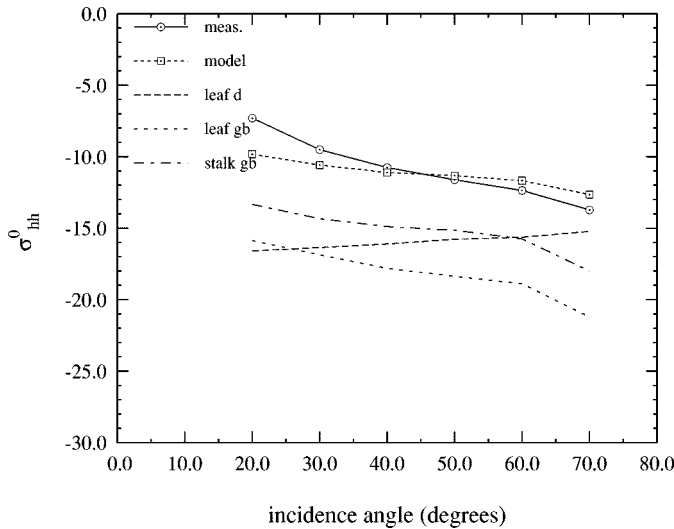
This behavior is demonstrated in Fig. 5, showing the measured and modeled data (σ_{vv}^0) for a wheat canopy prior to the emergence of the grain head. For the lower incidence angles, the scattering is dominated by the scattering mechanisms involving a “ground-bounce,” while the direct scattering component remains small. As the incidence angle increases, the electric field of the vertically polarized incident wave increasingly couples into the vertical structure of the wheat plant. This has two effects. One, the ground-bounce terms are rapidly attenuated with increasing incidence angle, diminishing this scattering mechanism to insignificance at 50°. Second, the direct scattering from the grain and the upper portion of the stalk increases, reaching the highest value at 70°. The combination of these two effects causes the dip in the measured response with the minimum backscattering occurring in the 40°–50° region.

Note the data presented for C-band in Fig. 5 correspond to the early test days before the grain head emerged from the stalk. After the grain head emerges, the model shows that this single grain element dominates the overall scattering from the wheat plant, with the direct grain scattering term the more significant for σ_{vv}^0 and the grain ground-bounce term the greatest for σ_{hh}^0 . Unfortunately, the simple scattering model used for the grain element did not provide the desired level of accuracy (both for extinction and scattering), and therefore the numerical match between model and measurement for the later test cases at C-band and X-band are not particularly satisfying, as demonstrated in Fig. 6.

Finally, recall that both the cross-section shape as well as leaf curvature are considered in the leaf scattering model. The first test day provides an excellent opportunity to examine the im-



(a)

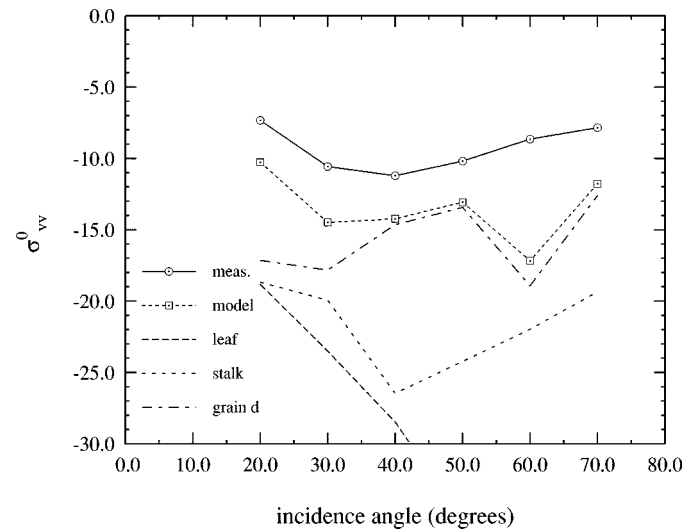


(b)

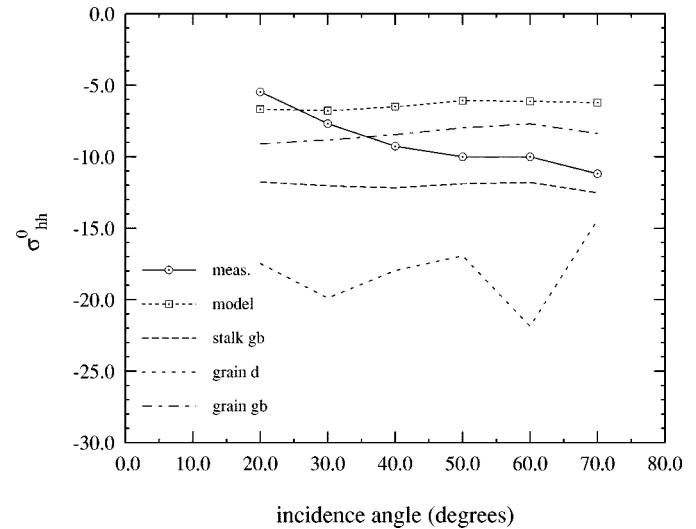
Fig. 5. C-band measured and modeled backscattering (σ_{vv} and σ_{hh}) from a short, green wheat canopy (May 25), plotted as a function of incidence angle. The direct scattering mechanisms are denoted as "d," the ground-bounce mechanisms as "gb."

portance of this added fidelity. The model shows that the scattering from the leaf elements dominate the horizontal copolarized case, a result due largely to the fact that the stalk element is the shortest on this test date. Additionally, as shown in Fig. 7(a), the model data match the measured data well and show that the direct leaf scattering is the largest scattering component, followed by the leaf ground-bounce terms, and then finally by the stalk ground-bounce terms.

Instead of using the leaf scattering model that considers cross-section and curvature, the data were again computed with leaves of the same cross-sectional area, average length, and angular distribution as before. However, this time, the cross section was assumed to be circular and the leaves to be straight. These results are provided in Fig. 7(b) and graphically demonstrate the tremendous difference between the two cases. For the straight, circular model, the direct leaf scattering drops by as much as 25 dB, with the leaf ground-bounce term likewise reduced by approximately 5 dB. Conversely, the stalk ground bounce has increased 2–3 dB and has thus been moved from the



(a)

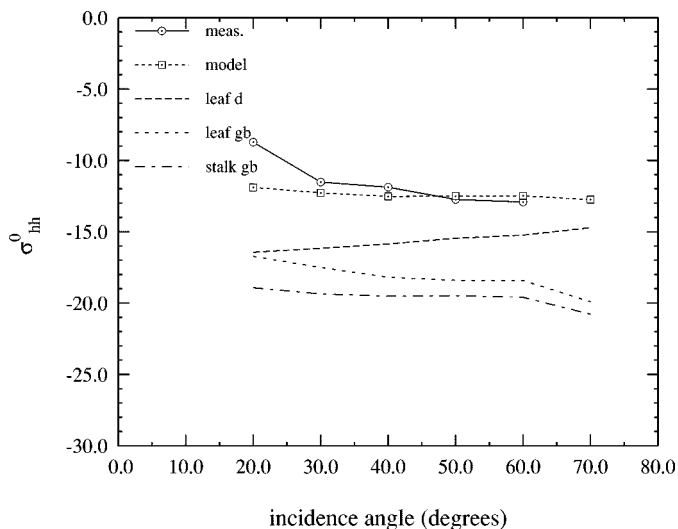


(b)

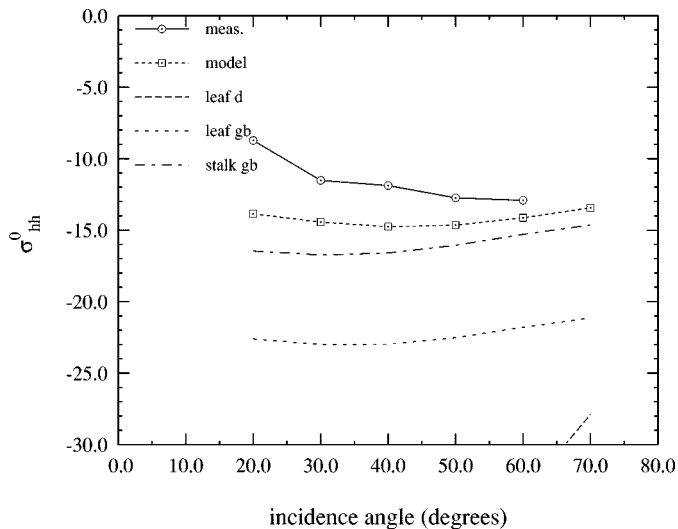
Fig. 6. C-band measured and modeled backscattering (σ_{vv} and σ_{hh}) coefficient for a test day after the grain head has fully emerged. The numerical error is associated with the dominance of the grain scattering, a plant element that is modeled with an inadequate scattering model. The direct scattering mechanisms are denoted as "d" and the ground-bounce mechanisms as "gb."

least significant scattering mechanism to the most significant. Making the leaf straight and circular not only changes the scattering attributed to leaf elements but to the scattering from stalks as well, because the extinction due to the leaf elements is also modified by this change of modeled shape and structure. This experiment indicates that the structure (in addition to dielectric and volume) is critical for accurately modeling grassland elements. Unlike trees, which can be modeled as complex, random collections of basic elements, grass plants are simpler and significantly less random structures. To a certain extent, this makes the modeling of these structures more difficult, as this basic structure must be reflected in the model.

A result of accurately modeling the constituent elements is that for this analysis, the model never predicts a significant contribution by the rough soil surface, even for small incidence angles, low frequencies (e.g., L-band), and low loss canopies. The backscattering coefficient for the rough soil (after accounting for the extinction of the vegetation) is at least 10 dB less than backscat-



(a)

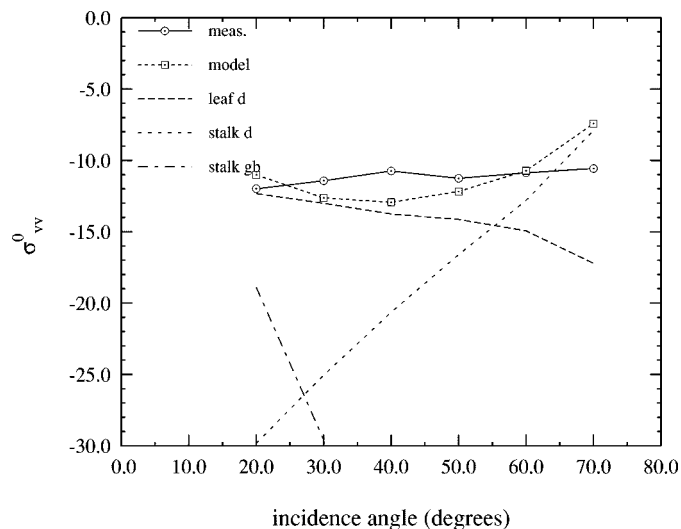


(b)

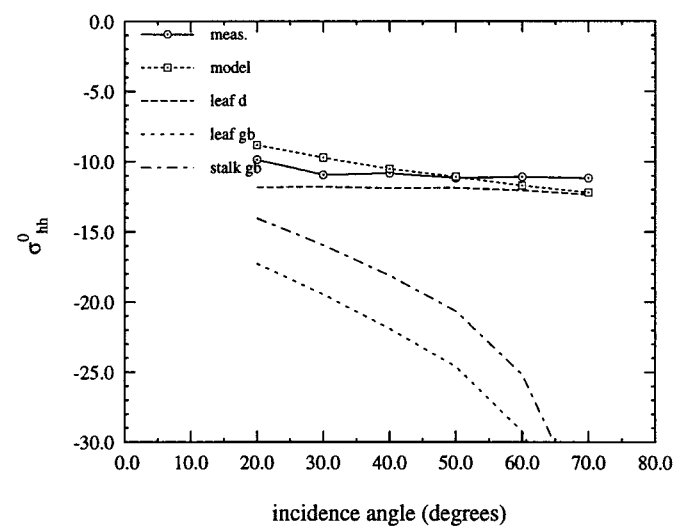
Fig. 7. Measured and modeled backscattering coefficient σ_{hh}^0 at C-band, evaluated with both the full leaf-scattering model (a) and a model assuming straight leaves of circular cross-section (b). The direct-scattering mechanisms are denoted as “d” and the ground-bounce mechanisms as “gb.”

tering from the vegetation. This is a different result than some interpretations of grassland and wheat scattering [10]. This disparity is due to the fact that both the extinction and scattering from curved and noncircular cross-section elements are significantly greater than that provided by straight, circular element models. Although the surface scattering predicted by the rough-surface model [13] is significant, the model shows that this scattered energy is attenuated by the canopy to the point of insignificance when compared to the scattering from the vegetation. This is not to say that the scattering response is independent of soil moisture, as the single-bounce terms of the first-order scattering model can in fact dominate the response and of course are dependent on the specular scattering from the soil surface. However, the diffuse scattering from the rough surface appears to have little effect on the overall canopy response. Of course, it is very difficult to make a general statement, as the soil observed in this experiment was relatively smooth and the vegetation is comparatively dense.

Since they are measured at a higher frequency, the coherent scattering terms at X-band will be even more insignificant than



(a)



(b)

Fig. 8. X-band measured and modeled backscattering (σ_{vv} and σ_{hh}) from a short, green wheat canopy (May 25), plotted as a function of incidence angle. The direct-scattering mechanisms are denoted as “d” and the ground-bounce mechanisms as “gb.”

for C-band, and thus, only incoherent backscattered power is considered at this frequency. Likewise, the large modeling errors exhibited in C-band when the grain head was present also occurred in the X-band data. The model does indicate, however, that the grain head is the dominant scatterer at X-band, with the direct scattering dominant for σ_{vv}^0 , and the ground-bounce mechanism similarly dominant for σ_{hh}^0 . For the early growth data (prior to the emergence of the grain), the model provided good results (Fig. 8), demonstrating that at X-band, the direct backscattering from the leaf element dominated for all incidence angles and for both copolarizations. This reflects the fact that the extinction through the canopy is significantly greater at X-band, and therefore, the ground-bounce scattering terms, with their long propagation path lengths, are diminished.

IV. CONCLUSIONS

It is apparent from the measured and modeled backscattering data that phase-coherent effects can have a significant or even dominant effect on the overall scattering at low frequencies. This

is particularly true for row-structured vegetation such as wheat, although correlation in the scattering from dissimilar plant elements can likewise have a profound effect. Thus, depending on the size and structure of the plant, in relation to the radar wavelength, the scattering from a single plant cannot be represented in terms of the scattering power from its individual constituent elements. Additionally, it was shown that the fidelity used to model the complex structure of the leaf elements is justified. The results from using circular, straight leaf elements, even those of identical length and volume, can result in profoundly different scattering predictions than the results from using the complex-leaf model.

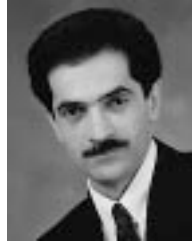
As frequency increases, the phase-coherent terms diminish. At these higher frequencies, the model predictions again match the measured data well and show the great difference in the scattering mechanisms between σ_{vv}^0 and σ_{hh}^0 data. However, the model does a poor job of predicting the measured scattering for the cross-polarized cases, a result that is likely due to the absence of second-order scattering terms in the model. Likewise, at high frequencies, when the grain-head scattering dominates, the model performance is again poor and demonstrates the need for a better grain-scattering model. Otherwise, the phase-coherent model appears to be a useful tool for analyzing the scattering of grassland canopies. The results seem to justify the additional complexity of the model, including phase-coherent effects, plant-element fidelity, and nonuniform illumination effects.

REFERENCES

- [1] F. T. Ulaby, M. W. Whitt, and K. Sarabandi, "AVNA-based polarimetric scatterometers," *IEEE Antennas Propagat. Mag.*, vol. 32, pp. 6–17, Oct. 1990.
- [2] B. A. M. Bouman, "Crop parameter estimation from ground-based X-band (3-cm wave) radar backscattering data," *Remote Sens. Environ.*, vol. 37, no. 3, pp. 193–205, Sept. 1991.
- [3] —, "Multi-temporal, multi-frequency radar measurements of agricultural crops during the Agriscat-88 campaign in The Netherlands," *Int. J. Remote Sensing*, vol. 14, no. 8, pp. 1595–1614, May 1993.
- [4] T. F. Bush and F. T. Ulaby, "Remotely sensing wheat maturation with radar," Remote Sens. Lab., Dept. Elect. Eng. Comput. Eng., Univ. Kansas, Lawrence, KS, RSL Tech. Rep. 177-55, May 1975.
- [5] P. Ferrazzoli and S. Paloscia *et al.*, "Sensitivity to microwave measurements to vegetation biomass and soil moisture content: A case study," *IEEE Trans. Geosci. Remote Sensing*, vol. 30, pp. 750–756, July 1992.
- [6] O. Taconet and M. Benallegue *et al.*, "Estimation of soil and crop parameters for wheat from airborne radar backscattering data in C and X bands," *Remote Sens. Environ.*, vol. 50, pp. 287–294, Dec. 1994.
- [7] U. Wegmuller, "Signature research for crop classification by active and passive microwaves," *Int. J. Remote Sens.*, vol. 14, pp. 871–883, Mar. 1993.
- [8] S. Bakhtiari and R. Zoughi, "A model for backscattering characteristics of tall prairie grass canopies at microwave frequencies," *Remote Sens. Environ.*, vol. 36, no. 2, pp. 137–147, 1991.
- [9] S. S. Saatchi, D. M. Le Vine, and R. H. Lang, "Microwave backscattering and emission model for grass canopies," *IEEE Trans. Geosci. Remote Sensing*, vol. 32, pp. 177–186, Jan. 1994.
- [10] A. Toure, K. P. Thompson, G. Edwards, R. J. Brown, and B. G. Brisco, "Adaptation of the MIMICS backscattering model to the agricultural context—Wheat and canola at L and C bands," *IEEE Trans. Geosci. Remote Sensing*, vol. 32, pp. 47–61, Jan. 1994.
- [11] J. van Zyl, "On the importance of polarization in radar scattering problems," Ph.D. diss., California Institute of Technology, Pasadena, Dec. 1985.
- [12] F. T. Ulaby, R. K. Moore, and A. K. Fung, *Microwave Remote Sensing: Active and Passive*. Norwood, MA: Artech House, 1985, vol. III.
- [13] Y. Oh, K. Sarabandi, and F. T. Ulaby, "An empirical model and an inversion technique for radar scattering from bare soil surfaces," *IEEE Trans. Geosci. Remote Sensing*, vol. 30, pp. 370–381, Mar. 1992.

James M. Stiles (S'91–M'95–SM'97) was born in Kansas City, MO, on June 4, 1961. He received the B.S. degree in electrical engineering from the University of Missouri, Columbia, in 1983, the M.S. degree in electrical engineering from Southern Methodist University, Dallas, TX, in 1987, and the Ph.D. degree in electrical engineering from the University of Michigan, Ann Arbor, in 1996.

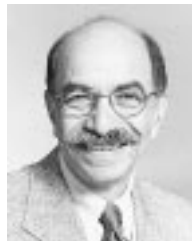
From 1983 to 1990, he was a Microwave Systems Design Engineer with Texas Instruments, Dallas, and from 1990 to 1996, he was a Graduate Research Assistant in the Radiation Laboratory, University of Michigan. Since 1996, he has been an Assistant Professor at the University of Kansas, where he is a Member of the Radar Systems and Remote Sensing Laboratory. His research interests include radar remote sensing of vegetation, propagation and scattering in random media, ground penetrating radar, and radar signal processing.



Kamal Sarabandi (S'87–M'90–SM'93–F'00) received the B.S. degree in electrical engineering from Sharif University of Technology, Tehran, Iran, in 1980 and the M.S.E. degree in electrical engineering, the M.S. degree in mathematics, and the Ph.D. degree in electrical engineering, in 1984, 1989, and 1989, respectively, from the University of Michigan, Ann Arbor.

From 1980 to 1984, he worked as a Microwave Engineer in the Telecommunication Research Center, Iran. He is presently an Associate Professor in the Department of Electrical Engineering and Computer Science, University of Michigan. He has 18 years of experience with microwave sensors and radar systems. In the past eight years, he has served as the Principal Investigator and Co-Investigator on many projects sponsored by NASA, JPL, ARO, ONR, ARL, and GM all related in one way or the other to microwave and millimeter wave radar remote sensing. He has published many book chapters and more than 80 papers in refereed journals on electromagnetic scattering, random media modeling, microwave measurement techniques, radar calibration, application of neural networks in inverse scattering problems, and microwave sensors. He has also had more than 140 papers and invited presentations in national and international conferences and symposia on similar subjects.

Dr. Sarabandi is listed in *American Men & Women of Science* and *Who's Who in Electromagnetics*. He has been a member of the IEEE GEOSCIENCE AND REMOTE SENSING ADCOM since January 1998 and has served as the Chairman of the Geoscience and Remote Sensing Society, Southeastern Michigan chapter, from 1992 to 1998. He is also a member of Commission F of URSI and of The Electromagnetic Academy. He was a recipient of the 1996 Teaching Excellence Award, the 1997 Henry Russel Award from the Regent of The University of Michigan, and the 1999 GAAC Distinguished Lecturer Award from the German Federal Ministry for Education, Science, and Technology.



Fawwaz T. Ulaby (M'68–SM'74–F'80) received the B.S. degree in physics from the American University of Beirut, Lebanon, in 1964, and the M.S.E.E. and Ph.D. degrees in electrical engineering from the University of Texas, Austin, in 1966 and 1968, respectively.

He is currently with the University of Michigan, Ann Arbor, as the Vice President for Research and the R. Jamison and Betty Williams Professor of Electrical Engineering and Computer Science. His current interests include microwave and millimeter wave remote sensing, radar systems, and radio wave propagation. He has authored eight books and published over 400 papers and reports on these subjects.

Dr. Ulaby is the recipient of the Eta Kappa Nu Association's C. Holmes MacDonald Award as "An Outstanding Electrical Engineering Professor in the United States of America for 1975," the IEEE Geoscience and Remote Sensing Distinguished Achievement Award (1983), the IEEE Centennial Medal (1984), the American Society of Photogrammetry's Presidential Citation for Meritorious Science (1984), the Kuwait Prize in applied science (1986), the NASA Group Achievement Award (1990), and the University of Michigan Distinguished Faculty Achievement Award (1991). He has served as President of the IEEE Geoscience and Remote Sensing Society (1980–1982) and the General Chairman of several international symposia. He is a member of URSI Commission F and the National Academy of Engineering.